Methodology To Probe Subunit Interactions in Ribonucleotide Reductases[†]

A. Quamrul Hassan,[‡] Yongting Wang,[§,⊥] Lars Plate,[‡] and JoAnne Stubbe*[,§,‡]

Departments of Chemistry and Biology, Massachusetts Institute of Technology, Cambridge, Massachusetts 02139

Received July 3, 2008; Revised Manuscript Received September 16, 2008

ABSTRACT: Ribonucleotide reductases (RNRs) catalyze the conversion of nucleotides to deoxynucleotides, providing the monomeric precursors required for DNA replication and repair. *Escherichia coli* RNR is a 1:1 complex of two homodimeric subunits, α2 and *β*2. The interactions between α2 and *β*2 are thought to be largely associated with the C-terminal 20 amino acids (residues 356−375) of *β*2. To study subunit interactions, a single reactive cysteine has been introduced into each of 15 positions along the C-terminal tail of *β*2. Each cysteine has been modified with the photo-cross-linker benzophenone (BP) and the environmentally sensitive fluorophore dimethylaminonaphthalene (DAN). Each construct has been purified to homogeneity and characterized by sodium dodecyl sulfate polyacrylamide gel electrophoresis (SDS−PAGE) and electrospray ionization mass spectrometry (ESI-MS). Each BP-*β*2 has been incubated with 1 equiv of α2 and photolyzed, and the results have been analyzed quantitatively by SDS−PAGE. Each DAN-*β*2 was incubated with a 50-fold excess of α2, and the emission maximum and intensity were measured. A comparison of the results from the two sets of probes reveals that sites with the most extensive cross-linking are also associated with the greatest changes in fluorescence. Titration of four different DAN-*β*2 variants (351, 356, 365, and 367) with α2 gave a $K_d \approx 0.4$ *μ*M for subunit interaction. Disruption of the interaction of the α2–DAN-*β*2 complex is accompanied by a decrease in fluorescence intensity and can serve as a high-throughput screen for inhibitors of subunit interactions.

Ribonucleotide reductases (RNRs)[1] catalyze the conversion of nucleoside-5′-di- or triphosphates (NDPs or NTPs) to deoxynucleoside-5′-di- or triphosphates (dNDPs or dNTPs) in all organisms and thus provide the essential precursors for DNA replication and repair (*1, 2*). In *Escherichia coli*, the active RNR is a 1:1 complex (α2*β*2) of two homodimeric subunits (*3*−*5*). The α2 subunit binds both NDP substrates and the dNTP/ATP allosteric effectors that govern the specificity and rate of dNDP production. The *β*2 subunit houses the diferric tyrosyl radical (Y•) cofactor (*6, 7*) that is required to initiate the nucleotide reduction on α2, 35 Å removed (*8*). No structure of an active $\alpha_n\beta_n$ complex of any class Ia RNR is available (*9*). Thus, the molecular details of subunit interactions essential for understanding radical propagation across the subunit interface and allosteric regulation that triggers this propagation remains an important issue to resolve. This paper describes new methodology to gain insight about this interface.

Several structures of α2 and of *β*2 are available (*8, 10*−*13*), however, and have provided a framework for methodology design. *E. coli* α2 (761 residues) in complex with a peptide composed of residues 356−375 of the C-terminus of *β*2 (*E. coli β*2 has 375 amino acids) was crystallized and solved. In this structure, residues 358−375 of the peptide were visible (*8, 13*). The binding mode of this peptide was proposed to be indicative of how the C-terminal tail of *β*2 binds to α2. Many structures of *E. coli β*2 are also available. In all cases, only residues 1−340 are visible (*11, 12*), with the remaining 35 residues, including 358−375, being disordered. Thus, no structural information is yet available about residues 341−357 of *β*2 and their roles in mediating subunit interactions.

Based on the individual structures of α2 and *β*2, Eklund and co-workers generated a docking model of a 1:1 complex of α2*β*2 using shape complimentarily and charge compatibility (*8*). The model is the basis for the 35 Å distance proposed between the essential Y• (Y_{122}) in *β*2 and the active site cysteine (C_{439}) in α2. Recent pulsed electron−electron double resonance experiments support this long distance and the docking model (*14, 15*). An independent validation of the model through identification of α2*β*2 interaction sites is required to increase our understanding of this unique long-range radical transfer pathway and its control by allosteric effectors.

[†] This work was supported by an NIH grant (No. GM29595 to J.S.). A.Q.H. is an Anna Fuller fellow funded by David H. Koch Institute for Integrative Cancer Research at MIT.

* To whom correspondence should be addressed. Tel: (617) 253-1814. Fax: (617) 258-7247. E-mail: stubbe@mit.edu.

[‡] Department of Chemistry, Massachusetts Institute of Technology.

[§] Department of Biology, Massachusetts Institute of Technology.

[⊥] Present address.

[1] Abbreviations: RNR, ribonucleotide reductase; α2, ribonucleotide reductase large subunit; *β*2, ribonucleotide reductase small subunit; NDP, nucleoside diphosphate; NTP, nucleoside triphosphate; ATP, adenosine-5′-triphosphate; CDP, cytidine-5′-diphosphate; dNDP, deoxynucleoside-5′-diphosphate; dNTP, deoxynucleoside-5′-triphosphate; NADPH, reduced *β*-nicotinamide adenine dinucleotide phosphate; BPM, benzophenone-4-maleimide; BADAN, 6-bromoacetyl-2-dimethylaminonaphthalene; DAN, dimethylaminonaphthalene; BP, benzophenone; DAN-*β*2, DAN-labeled *β*2; BP-*β*2, BP-labeled *β*2; DAN-*β*2(V365C), DAN-labeled *β*2 at V365C; BP-*β*2(V365C), BP-labeled *β*2 at V365C; HU, *N*-hydroxyurea; Y•, tyrosyl radical; TR, thioredoxin; TRR, thioredoxin reductase; DTNB, dithio-bis(2-nitrobenzoic) acid; kan, kanamycin; PMSF, phenylmethylsulfonyl fluoride; TNB, 2-nitro-5-thiobenzoate.

10.1021/bi8012559 CCC: $40.75
Published on Web 11/14/2008

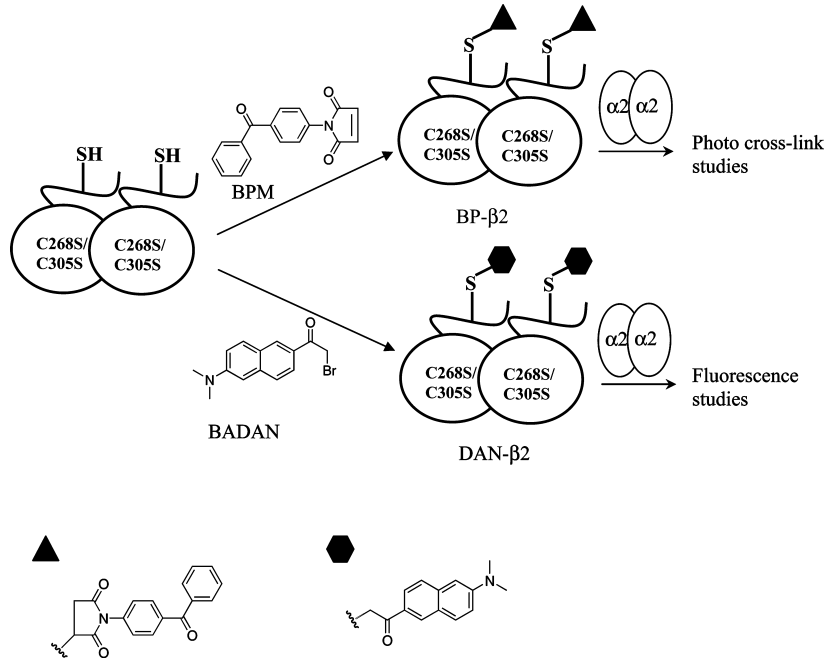

FIGURE 1: Strategy for site-specific labeling of β2. A single cysteine is placed within the C-terminal tail of β2 and then labeled with the photo-cross-linker (BP) or the environmentally sensitive fluorophore (DAN).

β is an obligate dimer (β2), while α is an equilibrium mixture of monomer and dimer (α2) with the dimer predominating in the presence of nucleotide (*3*). Interactions between α2 and β2 in all class I RNRs thus far examined are weak and largely dependent on the C-terminal 10−20 amino acids of β2 (*16*−*18*). The weak interaction, the potential changes in this interaction in the presence of substrates or allosteric effectors that bind to α2, and the consequences of these changes on enzymatic activity have prompted a number of studies to determine the K_d's for subunit interaction (*19*−*21*). Early studies used sucrose gradient ultracentrifugation and showed that allosteric effectors are required in the gradient for detection of $\alpha2\beta2$ complex formation (*4*). Inhibition studies with α2, β2, CDP, and ATP monitoring rate of dNDP formation using inactive β2 (Y122F) or using peptides of varying length corresponding to the C-terminus of β2 revealed a K_m of 0.2 μM for α2 and β2 (*18, 21*). Recently, surface plasmon resonance techniques were examined in an effort to determine the influence of allosteric effectors or substrates on subunit affinity (*20*). Unfortunately, technical problems in attaching β2 to the sensor chips have limited data interpretation. Thus, there is a gap in our quantitative understanding of complex formation between the subunits. Such information may well be important for the development of a quantitative description of allosteric regulation in class Ia RNRs in general and *E. coli* RNR specifically.

In the present paper, development of a method to probe subunit interactions is reported in which all surface-reactive cysteines in β2 are removed, and a single cysteine has been incorporated site-specifically into 15 positions in its C-terminal tail. Each cysteine mutant has been modified with the photo-cross-linker benzophenone (BP) to give a BP-β2 variant or with the environmentally sensitive fluorophore dimethylaminonaphthalene (DAN) to give a DAN-β2 variant (Figure 1). Analysis of cross-linking between α2 and BP-β2 by SDS−PAGE for all variants is reported, as are the fluorescent changes accompanying binding of DAN-β2 to α2. The results suggest that this method will be informative in acquiring molecular details and quantitative data about subunit interactions and the effects of substrates or effectors on these interactions.

MATERIALS AND METHODS

Materials. Benzophenone-4-maleimide (BPM) and 6-bromoacetyl-2-dimethylaminonaphthalene (BADAN) were purchased from Molecular Probes (Eugene, OR). BL21 Gold (DE-3) competent cells were purchased from Stratagene (La Jolla, CA). Isopropyl-1-thio-β-D-galactopyranoside (IPTG) and 1,4-dithiothreitol (DTT) were purchased from Promega (Madison, WI). Ni^{2+}-NTA resin was purchased from Qiagen (Valencia, CA). 1,10-Phenanthroline, 5,5′-dithio-bis(2-nitrobenzoic acid) (DTNB), *N*-hydroxyurea (HU), adenosine-5′-triphosphate (ATP), cytidine-5′-diphosphate (CDP), reduced β-nicotinamide adenine dinucleotide phosphate (NADPH), kanamycin (kan), and phenylmethylsulfonyl fluoride (PMSF) were purchased from Sigma (St. Louis, MO). DNase I and alkaline phosphatase were purchased from Roche Diagnostics (Indianapolis, IN). [5-^{3}H]Cytidine 5′-diphosphate, NH_4 salt (24.0 Ci/mmol), was obtained from GE Healthcare. The concentration of α2 was determined using $\varepsilon_{280} = 189\,000\ M^{-1}\ cm^{-1}$. α2 had a specific activity of 2500 nmol min^{-1} mg^{-1}. *E. coli* thioredoxin (TR) was isolated from the overproducing strain SK3981 and had a specific activity of 40 U/mg, and thioredoxin reductase (TRR) had a specific activity of 1800 U/mg (*22, 23*).

Methods. Construction of β2 Mutants. Site-directed mutagenesis was carried out using a QuickChange kit from Stratagene according to the manufacturer's protocol. pET15b-β2, which encodes $(His)_6$−β2(C268S/C305S), was used as a template for site-directed mutagenesis (*24*). Forward and reverse primers for the 15 mutants are listed in Supporting Information Table 1. Each β2 mutant was confirmed by DNA sequencing at the MIT biopolymer facility. All mutants are $(His)_6$-β2-C268S/C305S with a single additional mutation:

S341C, N343C, Q345C, A347C, Q349C, V351C, V353C, Y356C, V358C, I361C, V365C, T367C, L370C, F373C, and L375C.

Expression and Purification of β2 Mutants. A plasmid encoding each β2 mutant was transformed into competent BL21 Gold (DE-3) cells. The cells were grown on LB plates (50 μg/mL kan) and incubated at 37 °C overnight (~15 h). A flask containing 100 mL of LB (50 μg/mL kan) was inoculated with a single colony and incubated on a shaker at 37 °C overnight (~15 h). This subculture was then used to inoculate 2 × 2 L at a dilution of 1:200, and the cultures were incubated with shaking (200 rpm) at 37 °C. At an OD_{600} of ~0.7, a solution of 1,10-phenanthroline (prepared in 0.1 M HCl) was added to a final concentration of 0.1 mM (*25*). After 15 min, IPTG was added to a final concentration of 0.5 mM. The cells were grown for an additional 4 h and then harvested by centrifugation at 7000 × *g* for 20 min. A typical yield was 2.5 g/L of cell culture. An SDS−PAGE gel of the cell lysate before and after induction was run to confirm successful expression.

A typical purification involved suspension of the cell pellet in 5 mL of lysis buffer (50 mM Tris, 500 mM NaCl, 10 mM imidazole, pH 7.6) per gram of cells. PMSF stock was added to a final concentration of 200 μM. The cell suspension was homogenized, and the cells were lysed by a single passage with the French Press at 14 000 psi. DNase I (Roche, 10 U/μL per milliliter of lysate) was added, and the suspension was stirred for 10 min at 4 °C. The cell debris was removed by centrifugation (60 000 × *g*, 30 min). The supernatant was equilibrated with Ni^{2+}-NTA resin (3 mL of resin per gram of cells) by gentle stirring in a beaker for 1 h at 4 °C. The slurry was then loaded into a column and washed with 30 column volumes of lysis buffer. The bound protein was eluted with 200 mM imidazole in lysis buffer. The imidazole was removed by Sephadex G-25 column (2.5 × 25 cm, 20 mL) in 50 mM Tris, 5% glycerol, pH 7.6, and the protein fractions were pooled and concentrated to ~100 μM. The yield was typically 12.5 mg of apo β2 per gram of cell paste.

Reconstitution of the Diferric Y• Cofactor. The reconstitution and the determination of Y• content of each holo-β2 mutant spectrophotometrically using the dropline correction method was carried out as previously described (*26*).

Isolation and Prereduction of α2. The purification and prereduction of α2 were carried out as previously described (*27*). α2 was concentrated to 50 μM in the absence of DTT and stored in small aliquots at −80 °C.

Radioactive Assay of BP-β2 Variants. A typical assay was carried out in a final volume of 200 μL, which contained 50 mM *N*-2-hydroxyethylpiperazine-*N*′-2-ethanesulfonic acid (HEPES, pH 7.6), 15 mM $MgSO_4$, 1 mM EDTA, 0.1 μM BP-β2, 1.5 μM α2, 1 mM [^{3}H]-CDP (1093 cpm/nmol), 3 mM ATP, 1.0 mM NADPH, 30 μM TR, and 0.5 μM TRR. All the components except BP-β2 and the [^{3}H]-CDP were mixed together. The [^{3}H]-CDP was then added, and a 30 μL aliquot was removed for the zero time point. The reaction was initiated by the addition of BP-β2, and aliquots (30 μL) were removed over 4 min. All aliquots were quenched by the addition of 25 μL of 2% perchloric acid and neutralized by addition of 18 μL of 0.5 M KOH. The production of dCDP was analyzed using the method of Steeper and Steuart (*28*). One unit of RNR activity is defined as 1 nmol of dCDP production/min/mg.

Determination of Thiol Content of β2 Mutants Using DTNB. All buffers used were degassed in vacuo for at least 30 min and flushed with argon for 10 min immediately prior to use. In a typical measurement, DTT was added to β2 mutants (700 μL, 100 μM) to a final concentration of 10 mM, and the solution was incubated for 30 min at 4 °C. The protein was then passed through a Sephadex G-25 column (1 cm × 10 cm, 7 mL) equilibrated in degassed buffer A (50 mM HEPES, 1 mM EDTA, pH 8.0). The background spectrum of 25 μM DTNB in buffer A was recorded (A_{410} denoted as A1). The protein was then diluted to 10 μM in this buffer, and the background spectrum was taken (A_{410} denoted as A2). DTNB was added into the cuvette containing the protein to a final concentration of 25 μM, and the UV/vis spectrum was recorded until the reaction was complete (A_{410} denoted as A3). The concentration of 2-nitro-5-benzoate (TNB) and the β2 mutant in mM are given as follows [TNB] = (A3 − A2 − A1)/13.6 mM^{-1} cm^{-1} and [β2] = A_{280}/131 mM^{-1} cm^{-1}. The number of thiols/β2 is given by [TNB]/[β2].

Labeling of β2 Mutants with BPM. BPM (2.5 equiv from a 0.1 M stock solution in DMSO) was added to prereduced β2 (typically 500 μL, 75 μM) and was gently stirred at 4 °C for 30 min. The solution was then centrifuged to remove undissolved BPM and passed through a Sephadex G-25 column (2 cm × 25 cm, 40 mL) equilibrated in β2 buffer (50 mM Tris, 5% glycerol, pH 7.6). The DTNB assay was performed immediately after the Sephadex G-25 column (2 cm × 25 cm, 50 mL) to determine the extent of labeling. All BP-β2 variants were characterized before and after labeling by electrospray ionization mass spectrometry (ESI-MS).

Labeling of β2 Mutants with BADAN. BADAN (2.5 equiv from a 0.05 M solution in DMF) was added slowly to 150 μL of 45 μM prereduced β2 mutant with stirring at 4 °C. The solution was covered with foil to protect the reaction from light and stirred for 5 h. The BADAN was removed by centrifugation and Sephadex G25 column (2 cm × 25 cm, 40 mL) equilibrated in β2 buffer. A DTNB assay could not be used to determine the extent of labeling with BADAN because it has significant absorption at 410 nm (λ_{max} = 390 nm). The concentrations of DAN and β2 were determined using the following extinction coefficients: for β2, ε_{280} and ε_{390} are 131 mM^{-1} cm^{-1} and 12.2 mM^{-1} cm^{-1}, respectively, and for BADAN in H_2O (pH 7.6), ε_{280} and ε_{390} are 19.8 mM^{-1} cm^{-1} and 21 mM^{-1} cm^{-1}, respectively (Molecular Probes, Invitrogen). The calculation to determine stoichiometry of labeling is given by DAN/β2, which assumes that DAN attached to β2 has the same ε_{280} and ε_{390} as BADAN in solution.

ESI-MS Characterization of Labeled β2 Variants. Each sample for ESI-MS analysis was prepared immediately before analysis. β2 variant (15 μL of 50 μM) was exchanged into 0.1% trifluroacetic acid (TFA)/H_2O using a C18 ziptip (Millipore). The sample was then diluted to a final concentration of ~5 μM with 50% MeCN, 50% H_2O, and 0.1% TFA. Typically, 4−5 pmol of the diluted sample was injected into the Sciex triplequadrupole mass spectrometer (model API 365) at 5 μL/min via direct infusion, and data were collected in positive mode.

Photo-Cross-Linking Reaction between BP-β2 Variants and α2. To optimize the conditions for the photo-cross-linking reaction, an equimolar mixture of BP-β2 and α2 (0.5 μM, 2.5 μM, 5 μM, 7.5 μM) was incubated in 40 μL of 50 mM HEPES (pH 7.6), 15 mM $MgSO_4$, and 1 mM EDTA in 96-well plate (Corning, NY). The plate was positioned underneath a hand-held UV lamp (UVP, CA, equipped with glass filter) with a ~1.4 cm distance between the lamp and the surface of the protein solution. The protein was irradiated with the lamp (~365 nm) for 30 min at 4 °C. The protein from each solution was analyzed by 10% SDS−PAGE gel (2.5 μg of BP-β2, 5 μg of α2). The molecular weight and intensities of the cross-linked bands were calculated using Quantity One software (BioRad). The band intensities were normalized to the molecular weight of the cross-linked species (intensity I). In order to calculate the percentage of photo-cross-linking, the same amount of BP-β2 (2.5 μg) and α2 (5 μg) were also loaded onto the gel, and the intensities of the bands were normalized to the molecular weight to give intensity II and intensity III, respectively. The percentage of cross-linked product formed was calculated from (Intensity I)/(Intensity II + Intensity III). The percentage of cross-linked product for each variant was then normalized to BP-β2(V365C) to obtain the relative extent of photo-cross-linking.

Characterization of DAN-β2 Variants. Fluorescence studies of DAN-β2 variants were carried out on a QM-4-SE fluorimeter from Photon Technology International (Montreal, Quebec) using FELIX software and 2 nm excitation and 6 nm emission bandwidth slits. Measurements were performed at 22 ± 1 °C in an initial volume of 400 μL of 50 mM HEPES, 15 mM $MgSO_4$, 1 mM EDTA, pH 7.6, in 500 μL microcuvettes. The excitation wavelength was 390 nm, and the emission spectrum was obtained by scanning from 420 to 620 nm at a rate of 5 nm/s. A similar scan of the buffer was subtracted from all other scans. In a typical experiment, the fluorescence spectrum of DAN-β2 variant (0.1 μM, 400 μL) was recorded. Prereduced α2 was then added to DAN-β2 to a final concentration of 5 μM (50-fold excess), and the fluorescence spectrum was recorded. Assuming a K_d of 0.4 μM for subunit interactions, addition of 5 μM would result in >95% complex formation. The intensity integrated over the full spectrum (420−620 nm) in the presence of α2 (5 μM) was subtracted from the intensity in its absence to give relative intensity (I_r) for each DAN-β2 variant. The relative intensity (I_r) for each complex of α2−DAN-β2 was normalized to α2–DAN-β2(V365C) to give a comparative measure of the fluorescence change.

Determination of K_d for Subunit Interactions. The fluorescence spectrum of the DAN-β2 variant (0.1 μM) in 50 mM HEPES, 15 mM $MgSO_4$, 1 mM EDTA, pH 7.6, at 22 ± 1 °C was recorded to obtain the initial intensity (I_0) at the emission maximum. Prereduced α2 (40.0 μM) was then added in aliquots to this solution. Size exclusion chromatography (*3*) and sedimentation velocity methods on α suggest that it is predominantly a dimer at low micromolar concentrations. Thus at 40.0 μM, α is likely to be a dimer. After each addition, the sample was mixed, allowed to equilibrate, and then scanned to obtain the intensity (I). The scan was repeated to ensure equilibration. Typically, 15−20 min was required for equilibration. Addition of α2 was continued until a saturation point was reached, and the spectrum was recorded to obtain the maximum intensity (I_{max}). To correct for the change in concentration, $I - I_0$ was multiplied by the appropriate dilution factor. The K_d is given by the following:

$$K_d = \frac{[\text{DAN-}\beta2]_f[\alpha2]_f}{[\alpha2\text{–DAN-}\beta2]} \quad (1)$$

where $[\alpha2]_f$ and $[\text{DAN-}\beta2]_f$ are the free concentration of α2 and DAN-β2, respectively. The above expression for K_d assumes a 1:1 interaction between α2 and DAN-β2 (*3*) and can be reformulated as

$$F = \frac{[\alpha2]_f}{K_d + [\alpha2]_f} \quad (2)$$

where F is the fraction of DAN-β2 complexed with α2 (i.e., $[\alpha2\text{−DAN-}\beta2]/[\text{DAN-}\beta2]_{total}$) and $[\alpha2]_f$ is given by $[\alpha2]_{total} - F[\text{DAN-}\beta2]_{total}$. F is obtained from eq 3 (*29, 30*).

$$\frac{I - I_0}{I_{max} - I_0} \quad (3)$$

A nonlinear least-squares fit of the plot of F vs $[\alpha2]_f$ using prism (Graphpad) gave the K_d.

*Synthesis of Peptides Ac-YLVGQIDSEVDTDDLSNFQL (**1**) and Ac-IDSEVDTD (**2**).* The peptides **1** and **2** were made by solid phase peptide synthesis as previously described (*24*). Each product was characterized by HPLC and MALDI-TOF.

*Determination of Binding of **1** and **2** to α2.* In a final volume of 400 μL, the reaction mixture contained 0.1 μM DAN-β2(V365C), 0.1 μM α2, 1 mM CDP, 1 mM ATP, 50 mM HEPES, 15 mM $MgSO_4$, 1 mM EDTA, pH 7.6, at 22 ± 1 °C. The fluorescence spectrum of the above solution was recorded. Titration with **1** (2 μM to 1.0 mM) was carried out as described in the preceding section, and fluorescence intensity (I) was recorded until no further changes were observed. The intensity (I) was plotted against log[peptide], and the IC_{50}, the concentration of peptide required to obtain the half-maximal point of the titration, was determined using prism (Graphpad). This IC_{50} was then used to calculate the K_i from the following equation (*31*):

$$K_i = \frac{IC_{50}}{1 + \dfrac{[\text{DAN-}\beta2(\text{V365C})]_{total}(y_0 + 2)}{2K_d(y_0 + 1)} + y_0} + K_d\frac{y_0}{y_0 + 2} \quad (4)$$

where K_d is 0.06 μM and y_0 is the ratio of $[\text{DAN-}\beta2(\text{V365C})]_{bound}$ to $[\text{DAN-}\beta2(\text{V365C})]_{free}$ in the absence of the peptide. Equation 4 is a modified form of the Cheng−Prusoff equation (*32*). Use of this equation (*31*) requires that the peptide is a competitive inhibitor of β2 binding to α2 and that there are two peptide binding sites on α2, one per α, that are independent of each other (*18*).

RESULTS

Site-Specific Attachment of Photo-Cross-Linker and Fluorescent Probes To Study Subunit Interactions. Small molecule probes have been shown to provide important tools to study protein−protein interactions (*33*). The two probes chosen to study the interactions between α2 and β2 are the

photo-cross-linker BP (*34*) and the environmentally sensitive fluorescence probe DAN (*35*). BP can potentially allow covalent attachment of the BP-modified residue in β2 to one or more residues in α2 in the $\alpha2\beta2$ complex. The DAN probe in the appropriate position, on the other hand, has the potential to allow quantitation of the subunit interactions.

Theoretically, these probes could be incorporated into either α2 or β2. However, α2 contains 11 cysteines, 5 of which are essential for catalysis. Thus, generation of α2 with a single reactive cysteine, the method chosen for probe attachment, would be challenging. These challenges and the previously demonstrated importance of residues 356−375 of β2 for interaction with α2 (*18, 21*) thus suggested that attachment of probes within this sequence would provide the best choice to study subunit interactions. An examination of the structure of β2 reveals that it has five cysteine residues and that C268 and C305 are surface-exposed (*11, 12*). These cysteines are remote from the proposed $\alpha2\beta2$ interface, and consequently, attachment of probes to these sites are unlikely to be good reporters of subunit interactions (*8*). We have previously shown that the double cysteine to serine mutation (C268S/C305S) had no effect on the enzymatic activity of *E. coli* RNR (*36*), and this double mutant was chosen as the starting point for all further constructs. Using β2-C268S/C305S, we incorporated a single surface-exposed cysteine site-specifically into β2 through mutagenesis. Given the requirement of the C-terminal tail of β2 for interaction with α2, probe placement within this region is likely to report on this interaction. Moreover, because the C-terminal tail of β2 is unstructured and flexible (*37, 38*), cysteine introduced in this region will likely be accessible for labeling with thiol reactive probes. Our strategy is summarized in Figure 1.

Selection of the Residues for Probe Attachment. The crystal structure of α2 in complex with the 20 residue C-terminal peptide of β2 (356−375) guided the selection of residues for probe attachment (*8, 13*). Eighteen residues (358−375) of the peptide are visible. The structure shows that the majority of the peptide adopts a reverse turn configuration and is sandwiched between helix αI and α13. The side chains of residues V358, I361, V365, T367, L370, F373, and L375 of the peptide are projected toward α2. Each of these residues was, therefore, mutated to a cysteine and then labeled with BP and DAN. Because no information is available about residues 341−357, cysteine mutations were arbitrarily placed at every other position within this region. These 15 residues were selected for probe attachment.

Generation and Characterization of β2 Mutants. The cysteine mutations were introduced by site-directed mutagenesis using N-terminal $(His)_6$-tagged *nrdB* (N-terminal GHHHHHHM-β2) with C268S/C305S mutations as the template (Supporting Information, Table 1). The $(His)_6$ tag facilitated the rapid purification of the mutants and does not have any significant effect on the enzymatic activity (*24*). The growth of *E. coli* and expression of the mutants were carried out in the presence of the iron-chelator 1,10-phenanthroline resulting in purification of all 15 mutants in the apo form (*25*). The diferric $Y^{\bullet}$ cofactor was then reconstituted *in vitro* by standard procedures (*26*). The yield and the radical content of reconstituted holo mutants suggest that these cysteine mutations had little effect on the expression level of the protein or the assembly of the active cofactor (Supporting Information, Table 2). Assay with Ellman's reagent (DTNB) showed that each mutant had 1.9−2.1 surface-accessible thiols/β2. Activity assays with the cysteine mutants showed that the mutation in general reduced activity from 6000 nmol/min/mg (observed for the wt-β2) to 11−2586 nmol/min/mg (0.2−43% of the wt-β2 activity) depending on the location within the tail (Table 2). In the following sections, a specific β2 mutant such as $(His)_6$-β2-C268S/C305S/V365C is denoted as β2(V365C).

Table 1: K_d's for the Interaction between DAN-β2 Variants and α2 Determined by Fluorescence Titration[a]

DAN-β2 variant	K_d (μM)
DAN-β2(V351C)	0.38 ± 0.06
DAN-β2(Y356C)	0.41 ± 0.06
DAN-β2(V365C)	0.36 ± 0.07
DAN-β2(T367C)	0.34 ± 0.07

[a] Conditions: 50 mM HEPES, 15 mM $MgSO_4$, 1 mM EDTA, pH 7.6, 22 ± 1 °C.

Table 2: Specific Activities of β2 Variants[a]

proteins	cysteine variants, nmol/mg/min	BP variants, nmol/mg/min	DAN variants, nmol/mg/min
β2(S341)	*b*	3.4	*b*
β2(N343)	1210	893.7	*b*
β2(Q345)	*b*	8.8	*b*
β2(A347)	*b*	8.4	*b*
β2(Q349)	*b*	4.7	*b*
β2(V351)	*b*	74	*b*
β2(V353)	300	28	*b*
β2(Y356)	11	4	6.8
β2(V358)	*b*	43	*b*
β2(I361)	1091	161	533
β2(V365)	1575	158	540
β2(T367)	2586	482	601
β2(L370)	*b*	209	*b*
β2(F373)	1168	1093	*b*
β2(L375)	*b*	297	*b*

[a] For comparison, wt-β2 has an activity of 5933.0 nmol/mg/min. The lower limit of activity detection is 0.6 nmol/min/mg. [b] Not determined.

Labeling of β2 Mutants with BP and DAN. BPM was chosen to attach the BP probe to β2 (Figure 1). The reaction conditions for the Michael addition between the thiolate of the mutant β2 and BPM were optimized by monitoring the reaction using the DTNB assay. A typical protocol involved incubation of 75 μM mutant β2 with 187 μM BPM at 4 °C for 30 min at which time the reaction was complete. Each BP-β2 was purified and characterized by ESI-MS. In each case, the presence of a peak with the expected mass (within the error of the method <20 ppm) for BP-β2 and the absence of a peak for unlabeled β2 supported stoichiometric labeling (Supporting Information, Table 3). Each mass spectrum also showed a second species with a mass of 170−180 Da greater than the expected mass of the BP-β2 variants (Supporting Information, Figure 1). This second species has been observed previously in the mass spectra of wt-β2, $(His)_6$-β2, and semisynthetic β2 (*24*). The basis for this increase in mass is not understood. In addition, each mutant was characterized for its ability to make deoxynucleotides using an assay with [^{14}C]-CDP (Table 2). BP modification in general reduced activity to 3−1100 nmol/min/mg (0.07−8.1% of the wt-β2 activity) depending on the location within the tail. The lower limit of activity detection was 0.6 nmol/min/mg; thus all mutants are active.

The labeling of the cysteine mutants with DAN was accomplished by S_N2 displacement of bromide from BADAN

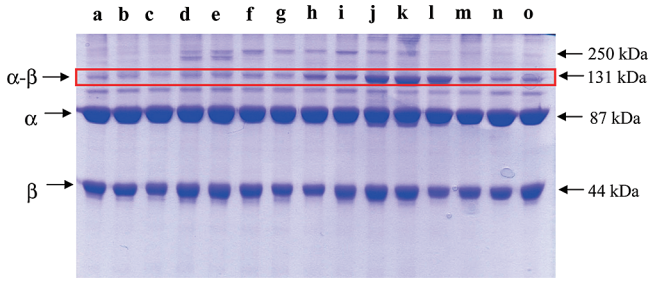

FIGURE 2: Photo-cross-linking reaction between each BP-β2 variant and α2. α (~87 kDa), BP-β variant (~44 kDa), and cross-linked product α−BP-β (131 kDa, box) are indicated with arrows. The band underneath the cross-linked product is a contaminant (~110 kDa) that copurifies with α2. A band corresponding to ~250 kDa is also shown. Each lane represents cross-linking of a different BP-β2 variant: (a) S341C; (b) N343C; (c) Q345C; (d) A347C; (e) Q349C; (f) V351C; (g) V353C; (h) Y356C; (i) V358C; (j) I361C; (k) V365C; (l) T367C; (m) L370C; (n) F373C; (o) L375C.

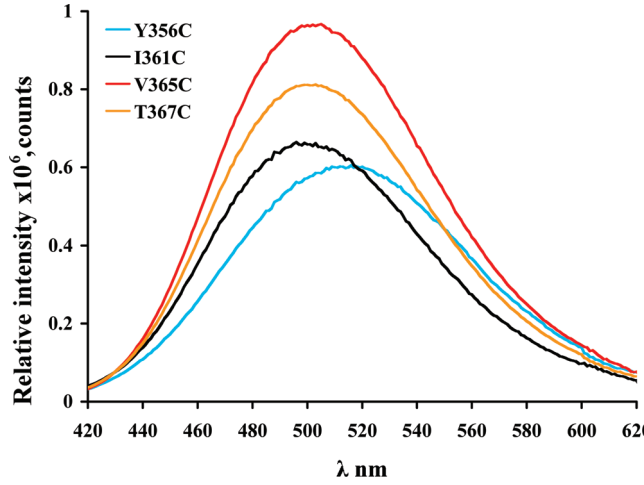

FIGURE 3: Fluorescence spectra of four DAN-β2 variants (0.1 μM) in complex with 5 μM of α2 in 50 mM HEPES, 15 mM $MgSO_4$, 1 mM EDTA, pH 7.6, at 22 °C. The excitation wavelength was 390 nm, and the emission spectra were collected from 420 to 620 nm.

by the cysteine thiolate. Optimized reaction conditions employed 75 μM β2 mutant with 2.5 equiv of BADAN at 4 °C for 5 h. Using the molar extinction coefficients of DAN and β2 at 280 and 390 nm, we determined the stoichiometry of DAN/β2 spectrophotometrically. It ranged from 1.9 to 2.2, with the variability likely due to the changes in DAN absorbance depending on its location within β2, relative to free DAN. The ESI-MS of variants 356, 361, 365, and 367 were determined and found to be identical to the expected values (Supporting Information, Table 4). As with the BP-β2 variants, additional mass of 170−180 Da was also observed with DAN-β2 variants. Activity assays of the four variants ranged from 0.1% to 13% of the wt-β2 (Table 2).

Photo-Cross-Linking Reaction between BP-β2 Variants and α2. To maximize the photo-cross-linking reaction between α2 and BP-β2 variants, the temperature, the time of exposure to light, and the subunit concentrations of α2 and BP-β2 were varied. In an optimized experiment, 5 μM α2 and BP-β2 were irradiated at ~365 nm for 30 min at 4 °C and then analyzed by SDS−PAGE. The results are shown in Figure 2. The molecular weights of α and BP-β are ~87 and 44 kDa, respectively and that of 1:1 complex of α−BP-β is ~131 kDa. The percentage of cross-linking was calculated by comparison of the intensity of the 131 kDa band with that of α and BP-β bands in the absence of light. This analysis shows that the yield of the photo-cross-linked product varies from 3% to 19%, with BP labeling at 361, 365, and 367 giving the highest yields (Supporting Information, Table 5). The location of Y356 is particularly important to establish given the absence of structural information, its essential role in radical propagation between α2 and β2, and the proposed distance of 25 Å between W48 in β2 and Y731 in α2 based on the docking model (*8*). The BP-β2(Y356C) variant shows ~9% cross-linking. BP variants in the region of 341−357 and at positions 373 and 375 near the C-terminus show 3−5% cross-linking. Efforts to increase the cross-linking efficiency by addition of substrate or effector to α2 and BP-β2 in which the $Y^{\bullet}$ was reduced were unsuccessful. Finally, in addition to the photo-cross-linked product observed at 131 kDa, a band of varying intensity with a molecular weight ~250 kDa was also present in BP-modified residues 347−365. The molecular weight analysis suggests that this band may be a complex of α2−BP-β2 (~260 kDa). A possible mechanism for its formation will be discussed subsequently.

Fluorescence Characterization of DAN-β2 Variants with α2. The fluorescence spectrum of each DAN-β2 variant was acquired in the presence of saturating amounts of α2, where the emission maxima ranged from 496 to 522 nm. The fluorescence spectra of a number of α2DAN-β2 variant complexes are shown in Figure 3. A comparison of the results shows differences in emission intensity, maxima, or both depending on the location of the probe (Supporting Information, Table 6). DAN-β2 (Y356, I361C, V365C, and T367C) show significant increases in fluorescence intensity with minimal change in emission maxima. DAN-β2(F375C), in contrast, shows both an increase in fluorescence intensity and a shift in emission maximum. Finally, DAN-β2(N343C and L345C) show very little change in fluorescence intensity or emission maximum.

Position-Dependent Comparison of the Extent of Photo-Cross-Linking and Change in Fluorescence of the β2 Variants. The percentage of photo-cross-linking and the change in fluorescence intensity of each BP-β2 and DAN-β2 variant were normalized to the values observed for β2(V365C), the variant with the largest changes in both cases (Figure 4). The extent of photo-cross-linking parallels the changes in fluorescence intensity, with the largest changes being observed in residues 361, 365, and 367. These studies suggest that 361−367 of the C-terminal tail of β2 might play an important role in subunit interactions. As discussed subsequently, competitive binding studies with peptides composed of these residues were carried out in an attempt to better understand the role of this region in subunit interactions.

Determination of K_d for Subunit Interactions with DAN-β2 Variants. The large increase in fluorescence intensity of DAN-β2(V365C) upon addition of α2 made this variant a good candidate to probe the binding affinity of α2 and β2, and thus DAN-β2(V365C) was titrated with increasing concentrations of α2 at 22 °C in the absence of allosteric effectors or substrates. As noted above, α in the absence of nucleotides is a mixture of dimers and monomers (*5*). Our titration experiments assume that α2 binds to β2 generating

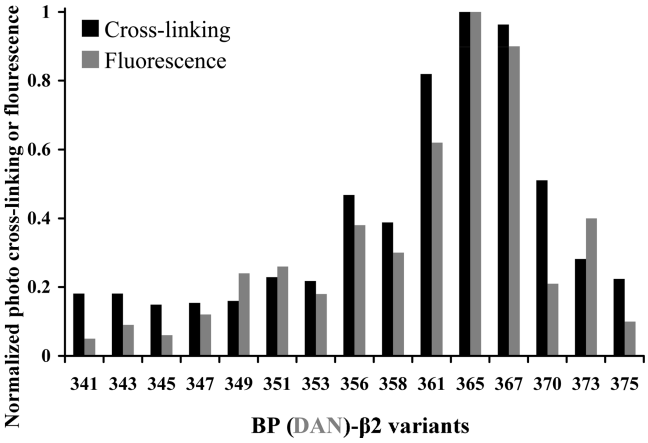

FIGURE 4: Comparison of the extent of photo-cross-linking reaction (black bars) of each BP-β2 variant relative to BP-β2(V365C) and fluorescence intensity (gray bars) of each DAN-β2 relative to DAN-β2(V365C).

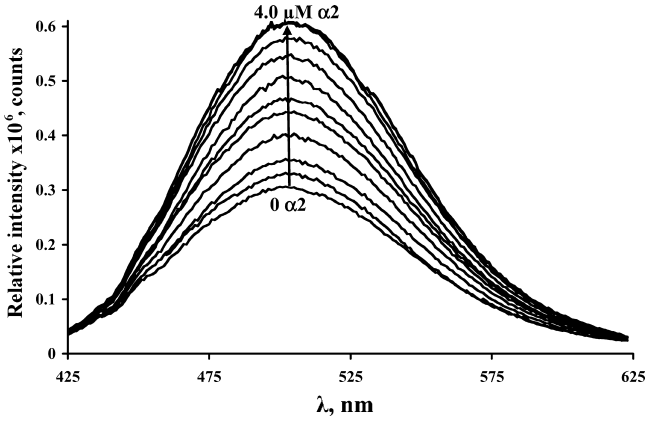

FIGURE 5: Fluorescence titration of DAN-β2(V365C) with increasing amounts of α2 (0−4.0 μM). Measurements were carried out in 50 mM HEPES, 15 mM $MgSO_4$,1 mM EDTA, pH 7.6, at 22 °C.

the $\alpha2\beta2$ complex and shifts the equilibrium of α to produce additional α2.

The results of a typical titration are shown in Figure 5. Analysis of these data gave a K_d of 0.36 ± 0.07 μM (Figure 6). The assumption has been made that at the end of the titration the predominant species is a 1:1 complex of α2 and β2. Modification of a residue involved in subunit interactions is likely to alter the measurement of interest. This alteration in the case of residue 365 is apparent from the reduced activity in nucleotide reduction (10 wt % activity). Thus, similar measurements were made with DAN attached to 351, 356, and 367. Residue 367 was chosen because of its similar behavior to 365 in the presence of α2 including its activity (Table 2). Residue 356 was chosen due to its importance in radical propagation between the subunits and the likely possibility that its position moves during binding and catalysis. Finally, residue 351 was chosen, because the previous studies with peptides to the C-terminal tail of β2 suggested that residues 340−355 have a small effect on subunit interactions (*18, 21*). Neither 356 nor 351 is observed in any crystal structure. Despite the different behaviors of these DAN-β2 variants, the titration studies surprisingly gave similar K_d's (Table 1). No previous studies have reported a quantitative assessment of $\alpha2\beta2$ interactions in the absence of nucleotides.

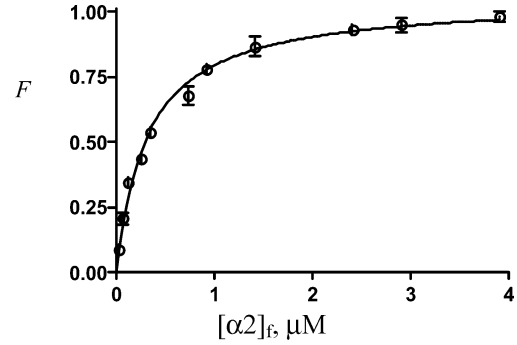

FIGURE 6: Plot of F vs $[\alpha2]_f$ to determine the K_d for $\alpha2$−DAN-β2(V365C) in the absence of substrate and effector. Measurements were carried out at 22 ± 1 °C in 50 mM HEPES, 15 mM $MgSO_4$, 1 mM EDTA, pH 7.6. Error bars are the standard deviation of three independent measurements.

Determination of K_d's for **1** *and* **2** *with* α2. The observed fluorescence changes upon $\alpha2$−DAN-β2 complex formation suggest a screen for inhibitors of subunit interactions and a way to assess the importance of residues 361−367 of β2 in this interaction. As proof of concept, we examined a peptide composed of residues Y356 to L375 of β2 with the N-terminus acetylated. This peptide was previously shown to inhibit subunit interaction with a K_i (equivalent to K_d) of 20 μM (*18*). The loss of fluorescence from the $\alpha2$−DAN-β2(V365) complex upon titration with increasing concentration of peptide should allow determination of its K_d.

In designing a fluorescence-based competitive assay, two factors are important (*29, 30*): the ratio between probe (DAN-β2) and receptor (α2) and the dynamic range of the assay, that is, the change in the signal (fluorescence intensity or polarization) between free and bound probe. The amount of α2 used in the assay was chosen to be 0.1 μM based on a K_d of 0.06 μM determined for the interaction of $\alpha2\beta2$ in the presence of substrate (CDP) and effector (ATP) (Hassan and Stubbe, unpublished results). The amount of β2 used (0.1 μM) was based on the intensity of the fluorescence changes (Figure 5) with this concentration of α2. As noted above titrations in the presence of nucleotides ensure α dimerization. Finally titrations were carried out in the presence of nucleotide to potentiate α dimerization. Increasing amounts of peptide **1** were added to $\alpha2$−DAN-β2(V365C) resulting in loss of fluorescence intensity at the emission maxima, ~503 nm. A plot of relative intensity vs log[**1**] allowed determination of the IC_{50} (Figure 7), which was then used to calculate K_i (equivalent to K_d) of 16.6 ± 2.7 μM (eq 4). The K_d for peptide **1** is ~40 fold higher than that for DAN-β2 variants. A difference of ~100 fold was found between the interaction of wt-β2 with α2 ($K_i = K_d = 0.2$ μM) and the interaction of the C-terminal peptide of β2 with α2 (residues 353−375, $K_d = K_i = 20$ μM) (*18*). Insight into the basis for the differences in K_d's between full-length β and the peptides was obtained from two independent studies where heterodimer of $\beta2$, $\beta\beta'$, (where β is full-length protein with residues 1−375 and β' is missing the last 22 amino acids or 24 amino acids) have K_d's of 6.5 μM (*18, 21*) and 11 μM (*39*). In addition, $\beta'\beta'$ showed no binding (*40*). These studies initially allowed Sjöberg and her co-workers to invoke a chelate effect, where binding of one β2 tail to α potentiates binding of the second tail to α (*18, 21*).

As noted above and summarized in Figure 4, there appears to be a correlation between sites resulting in the most

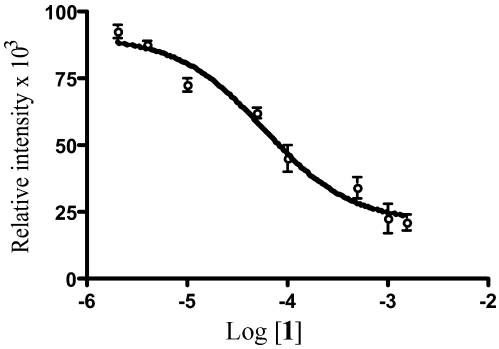

FIGURE 7: Plot of relative intensity vs log[**1**] to determine the IC_{50} of the peptide binding to α2. Measurements were carried out at 22 ± 1 °C in 50 mM HEPES, 15 mM $MgSO_4$, 1 mM EDTA, pH 7.6. Error bars are the standard deviation of three independent measurements.

extensive cross-linking and those associated with largest increases in fluorescence. Having established the validity of the competitive assay with **1**, an acylated octamer, **2** (Ac-IDSEVDTD), was synthesized to test the importance of these residues in the inhibition of subunit interactions. A titration with concentrations of **2** up to 10 mM peptide resulted in no loss in fluorescence intensity. Thus, this region by itself does not appear to be responsible for the predominant interactions with α2. This result might have been predicted from studies of Climent et al. (*18*) in which they determined K_ds for peptides corresponding to the C-terminus of *β* [peptide 1−8 (residues 368−375), 12−20 (residues 356−364), 1−19 (residues 357−375), 1−20 (residues 356−375) and 1−30 (residues 346−375)]. The acylated 8 mer (1−8) has a K_d of ∼400 *μ*M, while the 19 mer (1−19) has a K_d of 40 *μ*M. Only a difference of 10-fold is associated with residues 9−19. Thus, lack of binding of our peptide **2** (8−15) suggests once again, the importance of the chelate effect where binding of the C-terminus of *β* potentiates an additional small amount of binding associated with residues 8−15; without the C-terminus, thus no binding of **2** would be expected.

DISCUSSION

The present paper documents the site-specific incorporation of the photo-cross-linker (BP) and the environmentally sensitive probe (DAN) into intact *β*2 of RNR to probe subunit interactions. The studies with BP-*β*2 variants reveal that the cross-linking occurs to some extent at each site of BP attachment (Figure 2) with the highest extent of cross-linking occurring between 356 and 370. Photo-cross-linking efficiency for the catalytically important Y356 is observed, however, at only 9% efficiency. We have recently synthesized the [^{14}C]-iodoacetamide analog of benzophenone ([^{14}C]-BPI), and analyzed the cross-linking sites with *β*2(V365C) variant using trypsin digestion and Edman sequencing (*41*). Cross-links to 356 (either to α2 or within *β*2) are of particular interest because they might report on the flexibility of this residue during catalysis. The possibility of multiple interactions and the low level of cross-linking, however, will make this analysis challenging. An additional interesting observation from the cross-linking experiments is the presence of a higher molecular weight species (∼250 kDa) with BP-modified residues between 349 and 365. The nature of the complex is unknown, but the size suggests that the complex is composed of two α and two *β* units. A control photo-cross-linking experiment of BP-*β*2(V365C) in the absence of α2 was carried out. SDS−PAGE analysis showed the presence of only monomeric *β*, excluding the formation of an intersubunit cross-linking. To obtain a species with >250 kDa, one would need to assume that the cross-linking between α and *β* enhances the interaction for free α and *β* such that the complex is stable under SDS−PAGE conditions. Such a large molecular weight aggregate has recently been observed when gemcitabine diphosphate inactivates RNR (*3*). Further experiments are required to test the validity of the model.

DAN-labeled *β*2s were of interest for two reasons. First, the K_d's for the interactions between α2 and *β*2 in the presence of NDP substrates or dNTP effectors pairs have not been determined systematically (*18, 20, 21*). A quantitative model for allosteric regulation of RNRs must include an understanding of subunit interactions and the changes in the interactions in the presence of nucleotides. Second, fluorescence methods are now widely used in high-throughput screening (*29, 30*) to monitor inhibition of protein−protein interactions. Thus, DAN-*β*2 variants could also serve as a tool to find new antibacterial agents.

The DAN fluorophore was chosen as a probe because of its small size, high extinction coefficient, and environmentally sensitive properties (*35, 42*). In H_2O, DAN has an emission maximum of ∼550 nm, which blue shifts and shows an increase in intensity in a nonpolar environment. The docking model of α2*β*2 has, in part, been guided by the cocrystallization of α2 with a peptide corresponding to residues 356−375 of *β*2. The changes in fluorescence intensities and emission maxima are consistent with the hydrophobic environment that residues 361, 365, 367, 370, 373, and 375 encounter on binding based on the model (Supporting Information, Table 7).

To demonstrate the usefulness of the DAN-*β*2 variants for the determination of the K_d for subunit interactions and to assess the perturbation that might be affiliated with the probe, four different variants were chosen for fluorescence titration studies. Surprisingly, the measured K_d's for all four variants examined were almost identical (0.34−0.41 *μ*M). These numbers are 2-fold higher than the K_d's previously reported based on a kinetic analysis to determine K_i's for peptide inhibition (*18, 21*). However, in these experiments, the presence of CDP and ATP might account for the differences. Our studies suggest that DAN-*β*2 variants will be useful to quantitate the relative changes in subunit interactions in the presence of nucleotides. A quantitative and comprehensive analysis of the subunit interactions is a key component to a better understanding of allosteric regulation of RNRs and will be the subject of future reports.

The differences in the sequences of the C-termini of *β*2 from bacteria, viruses, and humans, the importance of subunit interaction in all cases for the formation of active RNR and the essentiality of RNR for cell survival suggest that subunit disruption could be a therapeutically important target (*17, 43*). Studies with peptidomimetics of the C-terminal tail of herpes simplex virus (HSV) RNR have been investigated as potential anti-HSV agents (*17, 43*), and peptides to the C-terminal tail of *β*2 from mouse RNR have been explored as potential anticancer agents (*17, 44*). A high-throughput screen of small molecule libraries could facilitate identification of lead compounds to inhibit α2*β*2 interactions and thus RNR

activity. Our preliminary data using a competitive fluorescence titration with **1** gave a K_d of 16.6 ± 2.7 μM, similar to the value previously determined by an independent method (*18*). Thus, monitoring fluorescence losses could provide a rapid high-throughput screening method for finding lead inhibitors.

SUMMARY

The methodology described in this manuscript offers new probes to determine the molecular basis for interactions between the subunits of RNR and to measure their affinities in the presence of different substrate and effector pairs. These methods can be readily extended to RNRs from other sources and should be generally useful for unraveling the complexities of these flexible proteins.

SUPPORTING INFORMATION AVAILABLE

List of primers used for mutagenesis experiments, the purification yield and radical content of β2 mutants, ESI-MS data for BP-β2 variants, ESI-MS data for DAN-β2 variants, the relative extent of photo-cross-linking of BP-β2 variants, fluorescence intensities and emission maxima of DAN-β2 variants, residues on α2 interacting with peptide 356−375 equivalent to the C-terminal tail of β2, and ESI-MS spectrum for BP-β2(V365C). This material is available free of charge via the Internet at http://pubs.acs.org.

REFERENCES

1. Stubbe, J., and van der Donk, W. A. (1998) Protein radicals in enzyme catalysis. *Chem. Rev. 98*, 705–762.
2. Jordan, A., and Reichard, P. (1998) Ribonucleotide reductases. *Annu. Rev. Biochem. 67*, 71–98.
3. Wang, J., Lohman, G. J. S., and Stubbe, J. (2007) Enhanced subunit interactions with gemcitabine-5′-diphosphate inhibit ribonucleotide reductases. *Proc. Natl. Acad. Sci. U.S.A. 104*, 14324–14329.
4. Brown, N. C., and Reichard, P. (1969) Ribonucleoside diphosphate reductase: Formation of active and inactive complexes of proteins B1 and B2. *J. Mol. Biol. 46*, 25–38.
5. Thelander, L. (1973) Physicochemical characterization of ribonucleoside diphosphate reductase from *Escherichia coli*. *J. Biol. Chem. 248*, 4591–4601.
6. Sjöberg, B. M., Reichard, P., Gräslund, A., and Ehrenberg, A. (1977) Nature of free-radical in ribonucleotide reductase from *Escherichia coli*. *J. Biol. Chem. 252*, 536–541.
7. Sjöberg, B. M., Reichard, P., Gräslund, A., and Ehrenberg, A. (1978) Tyrosine free-radical in ribonucleotide reductase from *Escherichia coli*. *J. Biol. Chem. 253*, 6863–6865.
8. Uhlin, U., and Eklund, H. (1994) Structure of ribonucleotide reductase protein R1. *Nature 370*, 533–539.
9. Uppsten, M., Farnegardh, M., Domkin, V., and Uhlin, U. (2006) The first holocomplex structure of ribonucleotide reductase gives new insight into its mechanism of action. *J. Mol. Biol. 359*, 365–377.
10. Eklund, H., Uhlin, U., Farnegardh, M., Logan, D. T., and Nordlund, P. (2001) Structure and function of the radical enzyme ribonucleotide reductase. *Prog. Biophys. Mol. Biol. 77*, 177–268.
11. Nordlund, P., and Eklund, H. (1993) Structure and function of the *Escherichia coli* ribonucleotide reductase protein R2. *J. Mol. Biol. 232*, 123–164.
12. Nordlund, P., Sjöberg, B. M., and Eklund, H. (1990) Three-dimensional structure of the free radical protein of ribonucleotide reductase. *Nature 345*, 593–598.
13. Eriksson, M., Uhlin, U., Ramaswamy, S., Ekberg, M., Regnstrom, K., Sjöberg, B. M., and Eklund, H. (1997) Binding of allosteric effectors to ribonucleotide reductase protein R1: reduction of active-site cysteines promotes substrate binding. *Structure 5*, 1077–1092.
14. Bennati, M., Robblee, J. H., Mugnaini, V., Stubbe, J., Freed, J. H., and Borbat, P. (2005) EPR distance measurements support a model for long-range radical initiation in *Escherichia coli* ribonucleotide reductase. *J. Am. Chem. Soc. 127*, 15014–15015.
15. Seyedsayamdost, M. R., Chan, C. T. Y., Mugnaini, V., Stubbe, J., and Bennati, M. (2007) PELDOR spectroscopy with DOPA-β2 and NH2Y-α2s: Distance measurements between residues involved in the radical propagation pathway of *Escherichia coli* ribonucleotide reductase. *J. Am. Chem. Soc. 129*, 15748–15749.
16. Cohen, E. A., Gaudreau, P., Brazeau, P., and Langelier, Y. (1986) Specific-inhibition of herpesvirus ribonucleotide reductase by a nonapeptide derived from the carboxy terminus of subunit-2. *Nature 321*, 441–443.
17. Cooperman, B. S. (2003) Oligopeptide inhibition of class I ribonucleotide reductases. *Biopolymers 71*, 117–131.
18. Climent, I., Sjöberg, B. M., and Huang, C. Y. (1991) Carboxyl-terminal peptides as probes for *Escherichia coli* ribonucleotide reductase subunit interaction - kinetic-analysis of inhibition studies. *Biochemistry 30*, 5164–5171.
19. Ingemarson, R., and Thelander, L. (1996) A kinetic study on the influence of nucleoside triphosphate effectors on subunit interaction in mouse ribonucleotide reductase. *Biochemistry 35*, 8603–8609.
20. Kasrayan, A., Birgander, P. L., Pappalardo, L., Regnstrom, K., Westman, M., Slaby, A., Gordon, E., and Sjöberg, B. M. (2004) Enhancement by effectors and substrate nucleotides of R1-R2 interactions in *Escherichia coli* class Ia ribonucleotide reductase. *J. Biol. Chem. 279*, 31050–31057.
21. Climent, I., Sjöberg, B. M., and Huang, C. Y. (1992) Site-directed mutagenesis and deletion of the carboxyl terminus of *Escherichia coli* ribonucleotide reductase protein R2 - effects on catalytic activity and subunit interaction. *Biochemistry 31*, 4801–4807.
22. Russel, M., and Model, P. (1985) Direct cloning of the trxB gene that encodes thioredoxin reductase. *J. Bacteriol. 163*, 238–242.
23. Lunn, C. A., Kathju, S., Wallace, B. J., Kushner, S. R., and Pigiet, V. (1984) Amplification and purification of plasmid-encoded thioredoxin from *Escherichia coli* K12. *J. Biol. Chem. 259*, 10469–10474.
24. Yee, C. S., Seyedsayamdost, M. R., Chang, M. C. Y., Nocera, D. G., and Stubbe, J. (2003) Generation of the β2 subunit of ribonucleotide reductase by intein chemistry: Insertion of 3-nitrotyrosine at residue 356 as a probe of the radical initiation process. *Biochemistry 42*, 14541–14552.
25. Baldwin, J., Krebs, C., Ley, B. A., Edmondson, D. E., Huynh, B. H., and Bollinger, J. M. J. (2000) Mechanism of rapid electron transfer during oxygen activation in the R2 subunit of *Escherichia coli* ribonucleotide reductase. 1. Evidence for a transient tryptophan radical. *J. Am. Chem. Soc. 122*, 12195–12206.
26. Bollinger, J. M., Tong, W. H., Ravi, N., Huynh, B. H., Edmondson, D. E., and Stubbe, J. (1995) Use of rapid kinetics methods to study the assembly of the diferric-tyrosyl radical cofactor of *Escherichia coli* ribonucleotide reductase, in. *Methods Enzymol. 258*, 278–303.
27. Mao, S. S., Holler, T. P., Yu, G. X., Bollinger, J. M., Booker, S., Johnston, M. I., and Stubbe, J. (1992) A model for the role of multiple cysteine residues involved in ribonucleotide reduction - amazing and still confusing. *Biochemistry 31*, 9733–9743.
28. Steeper, J. R., and Steuart, C. D. (1970) A rapid assay for CDP reductase activity in mammalian cell extracts. *Anal. Biochem. 34*, 123–130.
29. Kenny, C. H., Ding, W. D., Kelleher, K., Benard, S., Dushin, E. G., Sutherland, A. G., Mosyak, L., Kriz, R., and Ellestad, G. (2003) Development of a fluorescence polarization assay to screen for inhibitors of the FtsZ/ZipA interaction. *Anal. Biochem. 323*, 224–233.
30. Lasagna, M., Vargas, V., Jameson, D. M., and Brunet, J. E. (1996) Spectral properties of environmentally sensitive probes associated with horseradish peroxidase. *Biochemistry 35*, 973–979.
31. Munson, P. J., and Rodbard, D. (1988) An exact correction to the Cheng-Prusoff correction. *J. Recept. Res. 8*, 533–546.
32. Cheng, Y., and Prusoff, W. H. (1973) Relationship between inhibition constant (KI) and concentration of inhibitor which causes 50% inhibition (I50) of an enzymatic-reaction. *Biochem. Pharmacol. 22*, 3099–3108.
33. Imperiali, B., Shults, M. D., Vazquez, E., Rothman, D. M., Janes, K. A., Nguyen, A., Lauffenburger, D. A., and Yaffe, M. B. (2004) Chemical tools for the study of complex biological systems. *Mol. Biol. Cell 15*, 245A–245A.
34. Dorman, G., and Prestwich, G. D. (1994) Benzophenone photophores in biochemistry. *Biochemistry 33*, 5661–5673.
35. Farris, F. J., Weber, G., Chiang, C. C., and Paul, I. C. (1978) Preparation, crystalline-structure, and spectral properties of fluorescent-probe 4,4-bis-1-phenylamino-8-naphthalenesulfonate. *J. Am. Chem. Soc. 100*, 4469–4474.
36. Yee, C. S. (2004) Ph.D. Thesis, MIT, Cambridge, MA.

37. Lycksell, P. O., Ingemarson, R., Davis, R., Gräslund, A., and Thelander, L. (1994) 1H-NMR studies of mouse ribonucleotide reductase - the R2 protein carboxyl-terminal tail, essential for subunit interaction, is highly flexible but becomes rigid in the presence of protein R1. *Biochemistry 33*, 2838–2842.
38. Lycksell, P. O., and Sahlin, M. (1995) Demonstration of segmental mobility in the functionally essential carboxyl-terminal part of ribonucleotide reductase protein R2 from *Escherichia coli*. *FEBS Lett. 368*, 441–444.
39. Seyedsayamdost, M. R., and Stubbe, J. (2007) Forward and reverse electron transfer with the Y(356)DOPA-β2 heterodimer of *Escherichia coli* ribonucleotide reductase. *J. Am. Chem. Soc. 129*, 2226–2227.
40. Sjöberg, B. M., Karlsson, M., and Jornvall, H. (1987) Half-site reactivity of the tyrosyl radical of ribonucleotide reductase from *Escherichia coli*. *J. Biol. Chem. 262*, 9736–9743.
41. Hassan, A. Q., and Stubbe, J. (2008) Mapping the subunit interface of ribonucleotide reductase (RNR) using photo-cross-linking. *Bioorg. Med. Chem. Lett.*, in press.
42. Weber, G., and Farris, F. J. (1979) Synthesis and spectral properties of a hydrophobic fluorescent-probe - 6-propionyl-2-(dimethylamino)Naphthalene. *Biochemistry 18*, 3075–3078.
43. Liuzzi, M., Deziel, R., Moss, N., Beaulieu, P., Bonneau, A. M., Bousquet, C., Chafouleas, J. G., Garneau, M., Jaramillo, J., Krogsrud, R. L., Lagace, L., McCollum, R. S., Nawoot, S., and Guindon, Y. (1994) A potent peptidomimetic inhibitor of Hsv ribonucleotide reductase with antiviral activity *in-vivo*. *Nature 372*, 695–698.
44. Gao, Y., Tan, C., Kashlan, O. B., Kaur, J., and Cooperman, B. S. (2004) New peptide inhibitors of mammalian ribonucleotide reductase. Mechanisms of action. *Regul. Pept. 122*, 14–14.

BI8012559